IOSR Journal of Applied Physics (IOSR-JAP)
e-ISSN: 2278-4861.Volume 9, Issue 4 Ver. IV (Jul. – Aug. 2017), PP 04-12
www.iosrjournals.org

Influence of Co^{2+} ions on structural and magnetic properties of Co-precipitated Ni-Cr nanoferrite for cancer cell diagnosis and treatment

*S.Sukandhiya[1], B.Uthayakumar[2], S.Periandy[3]
[1,2](Research Scholar, Department of Physics, Kanchi Mamunivar center for PG Studies, Puducherry, India.)
[3](Associate Professor, Department of Physics, Kanchi Mamunivar center for PG Studies, Puducherry, India.)
* (Corresponding email id: sukandhiya2010@gmail.com)
Corresponding Author: * S. Sukandhiya

Abstract *Co^{2+} ions doped nano Nickel - Chromium ferrite (x= 0.0, 0.2, 0.4, 0.6, 0.8 and 1.0) synthesized by Co-Precipitation method with pH as 10. Prepared samples are sintered at 1173K. Influence of Cobalt ion on Structural and magnetic properties of $Co_xNi_{1-x}Fe_{1.5}Cr_{0.5}O_4$ nano ferrite were reported here. The structural parameters were estimated by X- ray Diffraction (XRD). Morphology and composition of the synthesized samples has been evaluated Scanning Electron Microscope (SEM) and Energy Dispersive X-ray Spectroscopy (EDX) respectively. The spinel formation have been investigated by Fourier Transform Infrared Spectroscopy (FTIR) and two prominent absorption bans ν_1 and ν_2 corresponding to the stretching vibration of tetrahedral and octahedral sites around 600 cm^{-1} and 400 cm^{-1}. The magnetic parameter such as Saturation magnetization (M_s), Remanent magnetization (M_r), Coercive field (H_c) and Squareness ratio are determined by Vibrational Sample Magnetometer (VSM). The xrd pattern shows synthesized nano powder samples are having cubic spinel structure with average crystallite size ranging from 39 to 60 nanometers. It is found that the lattice constant increase for increase in Co ions of Ni-Cr ferrite, lattice strain, and dislocation density value is is maximum for the concentration of x = 0.6, X-ray density is low for the concentration of x = 0.6.The magnetic parameters changes with respect to increase in concentration of Co^{2+} ions. Maximum Anisotropy obtained at x= 0.8 is 17219.49 (erg/cm^3).*

Keywords *- Co-Ni-Cr Ferrite, Co-Precipitation method, XRD, SEM, EDAX, FTIR, VSM*

Date of Submission: 02-08-2017 Date of acceptance: 14-08-2017

I. Introduction

Ferrites are a category of inorganic materials, cultivated more interest among the research community for the past few decades, due to their colossal properties. Nanoferrites are novel in comparison with the corresponding bulk part [1, 2] such as superparamagnetism, high surface area, large surface-to-volume ration and easy separation under external magnetic field and strong adsorption ability. They have burgeoning applications in electrical components, memory devices, magnetostriction, microwave devices and high-density magnetic recording [3 ,4]. Among the nanoferrites, spinel nanoferrites attracted researchers, because of their large magnetocrystalline anisotropy, moderate saturation magnetization, large magnetostrictive coefficient at room temperature, chemical stability, mechanical hardness, flexible magnetic properties[5-9] and the desired range of these parameters are tailored by chosen elements and composition . Generally magnetic nano particles have the potential to produce heat under an alternating magnetic field, this special property fascinated the researcher to do work on this field. During magnetization reversal, energy loss occurs this phenomenon paved the base for promising application of magnetic nano particles in biomedicine, known as Magnetic Fluid Hyperthermia MFH. MFH plays a vital role in thermal ablation therapy for cancer, since cancerous cells are more sensitive to heat than healthy one. MFH offers a better selectivity as heat is locally generated in the tissue where the magnetic nano particles accumulate. A strategy to achieve constant hyperthermic efficiency, by synthesizing novel combination of ferrite with increased magnetic anisotropy. Ragasudha et al,[10] synthesized Pure and Chromium doped Cobalt ferrite and successfully reported that addition of addition of Cr^{3+} ion with Cobalt ferrite has decrease the coercivity from 1760 to 338 Oe at room temperature, making the material magnetically very soft which will be suitable for high frequency transformers. Shakeel kahn et al, [11] investigated correlation of Cobalt substitution on the structural, electrical and optical properties of $Mn_{1-x}Co_xFe_2O_4$ (x = 0.0 to 0.5) prepared by sol-gel method and reported that lattice parameter decreases with increase in Co due to smaller ionic radius of Manganese in the composition. Ding Chen et al ,[12] prepared ball milled $Ni_xCo_{1-x}Fe_2O_4$ (x=0.2, 0.5, 0.8) with particle size 15 nm and reported increase in Nickel and decrease in cobalt content results in decreased values of coercivity (H_c) and saturation magnetization (M_s). The structure of

cobalt ferrite and nickel ferrite have inverse spinel with space group Fd3m which is based on an oxygen fcc sublattice in which Ni^{2+}, Co^{2+} and Fe^{3+} cations equally occupy the octahedral B sites, while the tetrahedral A sites are occupied by remaining Fe^{3+}. Moreover only an eighth of the tetrahedral sites are occupied by the Fe^{3+}, and only half of the 16 octahedral sites are occupied by the two Ni^{2+} and Fe^{3+} ions. This large fraction empty interstitial sites creates a very open structure that permits cation migration [13]. Presence of Non-magnetic Cr^{3+} ions with strong B site preference could produce sufficient changes in the structure of Nickel-Cobalt ferrite. Comprehensive literature survey has been done and a novel composition of Co-Ni-Cr nanoferrite (x = 0 to 1.0 in steps of 0.2) synthesized by co-precipitation method is not reported yet and in this paper we devoted to the influence of concentration of Cobalt on Nickel-Chromium ferrite employing co-precipitation method. Present investigation is to reveal the physio-chemical behavior with respect to Co^{2+} ion concentration.

II. Materials and Methods

2.1 Material for synthesis

$Co_xNi_{1-x}Fe_{1.5}Cr_{0.5}O_4$ nano ferrites at various concentration of Cobalt ion has been synthesized from Precursors $CoCl_2$, $NiCl_2$, $CrCl_3.6H_2O$, $FeCl_3.6H_2O$ and NaOH. Analytical grade of these precursors are purchased from SIGMA ALDRICH, Germany with 98% purity.

2.2 Synthesis Methodology

A fruitful synthesizing methodology involves correct choice of precursor, its composition and reaction environment. Particularly for wet chemical methods like sol-gel, hydrothermal, co-precipitation and colloid emulsion technique, pH controller plays an important role. For the present work eco friendly NaOH is used to maintain pH. The physio-chemical properties of nanoparticles are greatly influenced by particle size, morphology, purity and chemical composition. Using chemical methods, have been conformed to efficiently control the morphology and chemical composition of prepared nano powder. Among wet chemical techniques sol-gel, hydro thermal and colloid emulsions are time consuming and involve highly unstable alkoxides and difficult to maintain reaction conditions. Co-precipitation is one of the more successful techniques for synthesizing ultrafine nanoparticles having narrow particle size distribution [14].These advantages on co-precipitation method motivated authors to synthesize $Co_xNi_{1-x}Cr_{0.5}Fe_{1.5}$ (x = 0, 0.2, 0.4, 0.6, 0.8,1.0) nano ferrites by co-precipitation method. The precursors for Fe ion is taken as 2 M and 1M for other Metals chlorides. They are mixed in stochiometric ratio and added one by one on the basis of their electronegativity value. Mixture of Aqueous solution is stirred rigorously at 338K for 30 minutes, meanwhile NaOH is added to the brain solution by drop by drop using a burette till solution reaches pH value 10. The required composition of nano ferrites are formed from conversion of metal salt into hydroxide and then transformed into ferrites. The precipitates obtained were thoroughly washed more than three times with double distilled water and acetone. The final product were dried and sintered at 1173 K for the formation of spinel ferrite crystal structure.

2.3 Physical measurements

Crystal structure of all the samples were examined by powder X-Ray diffraction XRD patterns at room temperature PANalytical-X'Pert PRO powder diffractometer using Cu-$K_{\alpha 1}$ radiation. Scanning Electron Microscopy (SEM) study was performed by VEGA 3 TESCAN Scanning Electron Microscope, operated at 120 KV. Elemental analysis has been done with BRUKER EDS. Fourier Transform Infrared (FT-IR) spectra were recorded on SHIMADZ FT-IR spectrophotometer using KBr pellets in the range 4000-400 cm^{-1}. The magnetic properties were measured at room temperature by LAKESHORE vibrating sample magnetometer (VSM).

III. Result and Discussion

3.1 X - Ray Diffraction analysis

Fig.1 shows x-ray diffraction pattern of synthesized samples of Cobalt doped Nickel-Chromium nano ferrite for the concentration x = 0, 0.2, 0.4, 0.6, 0.8 and 1.0. Major peaks (220), (311), (400), (422), (511) and (440) are present in XRD pattern of all the samples which reveals these are having the disordered spinel ferrite formation of space group Fd3m, with Fe^{3+} in tetrahedral (8c) and octahedral (12d) sites whereas Ni^{2+} and Co^{2+} ions occupy the octahedral position[15]. This matches with the JCPDS file No.10-0325 and No.85-2456. In addition to major peaks, minor reflections peaks from the planes (222), (422), and (620) are present in all samples except x = 0.4, 0.6 and 1.0. This disappearance of minor reflection peaks are due to slight amorphization of sample.[16,17]. For these combination of samples no extra peaks are obtained which represents all samples are not ordered spinels . Generally intensity of XRD peaks corresponds to the crystalline nature of the samples. For undoped Ni-Cr nano ferrite, intensity of XRD peaks higher than all other samples. Addition of higher ionic radius Co^{2+} ion (r_{Co} = 0.74 Å) in Ni-Cr nano ferrite which will influences the crystalline nature of all samples and Increase in Cobalt concentration decreases the crystalline nature, which results in

decrease in XRD peak intensity. Intensity and peak width of XRD pattern related to particle size and crystallinity of the samples. The intensities of (220) and (440) planes are more sensitive to cations in tetrahedral and octahedral sites respectively. [18,19] From TABLE 1 it is clear that intensity of (440) increases with increase in Co^{2+} upto x = 0.4 this due to decrease in Nickel at octahedral site [20]. At 0.6 concentration (440) intensity drops abruptly this due to point of inversion of spinel structure. Intensity of 220 varies non linearly because of Presence Fe^{2+} ion in the octahedral site formed due to reduction of Fe^{3+} ion to Fe^{2+} ions for higher Cobalt concentration. Average crystallite size 'D' and lattice constant has been estimated from X-ray reflections indexed (111), (220), (311), (222), (400), (422), (511), (440) and (620), using Scherer's equation $D = 0.9 \lambda / \beta \cos \theta$, where D is the average crystallite size, β is the full width half maxima, λ is the X-Ray wavelength and θ is the Bragg's angle [7]. Lattice constant has been calculated from equation $a = d (h^2 + k^2 + l^2)^{1/2}$ Where 'a' is lattice constant, d be the inter planar distance, hkl is miller indices. Lattice strain of $Co_xNi_{1-x}Cr_{0.5}Fe_{1.5}O_4$ were determined using the Williamson-Hall formula $\varepsilon = \beta / 4 \tan \theta$, Where ε is the lattice strain of the structure [21, 22]. X-ray Density can be calculated by $\rho_x = ZM/Na^3$, Where Z is number of molecules per unit cell, here it is 8. M is Molecular weight of the sample N is Avagadro's Number, 'a' lattice constant. Dislocation density has been found by using the relation $\delta = 15 \varepsilon / a D$, here δ be the dislocation density. All these structural parameters are calculated and tabulated in TABLE 2. The average crystallite size 'D' estimated for $Co_xNi_{1-x}Cr_{0.5}Fe_{1.5}O_4$ nanoferrites for different 'x' values lie in between 39 nm and 60 nm. The samples having lattice constant between 8.4407 Å and 8.5410 Å and this increases in lattice constant with increase in concentration of Cobalt is due to addition of higher ionic radius Co^{2+} ion (r_{Co} = 0.74 Å) which replaces the smaller ionic radius Ni^{2+} ion (r_{Ni} = 0.69 Å) [23, 24]. Only $Co_{0.6}Ni_{0.4}Cr_{0.5}Fe_{1.5}O_4$ violates Vegard's law, this behaviour is due to point of inversion of mixed spinel, large dislocation (2.94×10^{15} lines/m) , most strained lattices (4.08×10^{-3}) and low X-ray density value. Increase in Co^{2+} concentration leads to increase in average crystallite size and lattice constant. Variation in the crystallite size is generally due to the influence of dopant, here crystallite size and lattice constant increase upto x = 0.4 concentration this. Ni^{2+} and Co^{2+} ions prefers octahedral sites whereas Fe^{3+} ions prefers both tetrahedral and octahedral sites. When the particle size reduced to nano dimension there is change in cation distribution Co^{2+} occupies both tetrahedral and octahedral sites [25]. For concentration x = 1 crystallite size is maximum with value of 60.3 nm. These phenomenon arise due to more strained and dislocated sublattice created by Cobalt. Molecular weight of the $Co_xNi_{1-x}Cr_{0.5}Fe_{1.5}O_4$ composition increases with replacement of higher atomic mass (58.93 gm) Co^{2+} by lower atomic mass (58.69 gm) Ni^{2+} in the composition and this matches with the X-Ray. density values calculated from XRD profile. Dislocation density value low for x=1 this is due to ordering nature of Co^{2+}.

3.2 Scanning Electron Microscope (SEM) and Energy Dispersive Spectroscopic (EDS) analysis

The morphological characteristics of the obtained $Co_xNi_{1-x}Cr_{0.5}Fe_{1.5}O_4$ nanoferrites sintered at 1173 K have been investigated with the help of VEGA 3 TESCAN for all concentration of the samples. Fig.2 shows morphology of $Co_xNi_{1-x}Cr_{0.5}Fe_{1.5}O_4$ nano ferrite samples for the increase in concentration of Cobalt (x = 0, 0.2, 0.4, 0.6, 0.8, 1.0). The micrographs show the agglomerated grain structure with clusters of fine particle clinging together. The morphology is almost uniform and regular having spherical shaped particles for all the concentration except 0.8. Replacement of Nickel by Cobalt manipulated the morphology. Agglomeration is more for $x \leq 0.4$ and this phenomenon is due to increase in magnetic interaction among the particles influenced by Co^{2+} [26]. Thus results of SEM well in agreement with X-Ray diffraction pattern. Especially for x = 0.4, 0.6, 1.0 agglomeration is more, this matches with disappearance of reflection planes (111), (222) and (620) due to amorphization and x = 0, 0.2, 0.8 morphology shows fine particle nature. The surface of the ferrite samples has a number of fine pores or voids that are attributed to the large amount of Oxygen and chlorine gas liberated during the sintering process. Presence of vacancies results in contraction of Lattice even higher ionic radius dopant is added to the sample. [27].

EDS spectrum for the $Co_xNi_{1-x}Cr_{0.5}Fe_{1.5}O_4$ (x = 0, 0.2, 0.4, 0.6, 0.8, 1.0) nanoferrites are recorded with BRUKER EDS and illustrated in Fig.3. The result shows each peak corresponds to the element added in the prepared nanoferrite which confirmed the presence of elements in respective concentration. Iron and oxygen are the major constituents in the composition and Chromium and cobalt is the next major constituent to the iron in the sample. It is interesting to note that the preparation condition completely favours the formation of mixed ferrite and allow us to study the effect of increasing the Co content on the properties of the Ni-Cr nano ferrite. The peak values variation is due to it stochiometry, for all the concentration. The values of Nickel vary with the increase in Cobalt concentration.

3.3. Fourier Transform Infrared Spectroscopy (FTIR) Analysis

Fourier transform infrared (FTIR) studies were carried out to ascertain the metal-oxygen bonding. FTIR spectrums of the investigated sample are shown in Fig.4. Infrared spectroscopy study supported the formation of Ni-Co-Cr spinel nano ferrite with enlightening two strong absorption bands around 400 cm^{-1} and

600 cm^{-1} that are common features of all spinel ferrites [28]. The spinel structure are attributed to the stretching vibrations of the unit cell of the spinel in the tetrahedral (A) Site and The metal-oxygen vibration in the octahedral (B) site. These absorption bands are highly sensitive to changes in interaction between oxygen and cations, as well as to the size of the obtained nano-particles [29]. The broadening of the spectral band depends on the statistical distribution of cations over A and B sites. The vibration frequency depends on the cation mass, cation-oxygen distance and bending force [30]. From Fig 4 and Table 3, Intrinsic stretching vibration frequency of metal- oxygen at tetrahedral site observed in a range 617 cm^{-1} - 601 cm^{-1} and its value shifting linearly toward lower frequency with increase in Co^{2+} concentration in the samples. And replacement of Ni^{2+} ions by bigger Co^{2+} in octahedral sites in Cobalt doped Nickel-Chromium ferrite results in a slight increase in metal oxygen bond length and consequently decrease the wave number of octahedral and tetrahedral sites by increasing substitution content [31, 32]. No octahedral peak observed in the range of 443cm^{-1} in concentration values of x= 0.6. Intensity of the peaks corresponds to octahedral and tetrahedral bonds increases for $x \leq 0.6$ and decreases for 0.8 and 1.0 concentration with the addition of Co^{2+} content. It is well known that the intensity ratio is function of change of dipole moment with the internuclear distance. This value represents the contribution of ionic bond Fe-O in the lattice. So the observed increase and decrease in the absorption band intensity with increase in Cobalt content, is due to perturbation occurring in Fe-O bonds. The electronic distribution of Fe-O bonds greatly affected by the dopant Co^{2+} which is having comparatively bigger radius and high atomic weight (Co- 58.93 amu , Ni 58.69 amu)[33].

3.4 Vibrational Sample Magnetometer (VSM) analysis

MH-loops reveals the magnetic properties of $Co_xNi_{1-x}Cr_{0.5}Fe_{1.5}O_4$ nanoferrites (x = 0, 0.2, 0.4, 0.6, 0.8, 1.0). Hysteresis loops for the samples are recorded with LAKESHORE Vibrational sample magnetometer at 300 K with applied field as 20 KOe are shown in Fig.5..The value of anisotropy constant was calculated from Stoner-Wohlfarth relation as follows $H_c = K/M_s$ [34] ,Where H_c is the coercivity , M_s saturation magnetization and K magnetic anisotropy constant .Calculation of magnetic moment in bohr magneton was carried out using the following relation, n_B = (Molecular Weight × M_S)/5585 [35]. Magnetic parameters saturation magnetization (M_s), Remanence Magnetization (M_r), Coercivity (H_c), Squareness ratio, Magnetic anisotropy constant (K) and magneton number are calculated from Hysteresis loop and tabulated in Table 4.Generally magnetic properties in the prepared sample arise from coupling between spin and orbital angular momentum (L-S coupling) and electron spin (S-S coupling) [36]. In the case of spinel nano magnetic ferrite material magnetic parameters are influenced by cation distribution, collinearity and non collinearity (canting) of spins on their surface, Crystallite size and dopant. In present study all the concentration of Co^{+}, the hysteresis loops show similar behaviour where the magnetization first increases abruptly with increase in the field up to 1000 Oe and then increase slowly and saturates ate nearly 2500 Oe of the applied magnetic field. From the graph Saturation magnetization value remains nearer to 31 emu/g for the concentration 0 to 0.4 of Co^{2+} and $x > 0.4$ M_s value increase. For inversion concentration 0.6 of mixed spinel having highest Saturation magnetization value i.e 80 emu/g due to most disordered spinel structure with more strain in the lattice, which will in agreement with XRD and SEM results. Coercivity varies non linearly due to the influence of Co^{2+} ion in the sample and variation in crystallite size. High value of coercivity is observed for higher concentration of Co^{2+} ion for all other concentrations Coercivity value is more. But Remanence value increase with increase in Co^{2+} ion. This is due to more number of incorporation of Co^{2+} ion on the sublattices . All the sample shows super-paramagnetic behaviour. The appearance of super-paramagnetism indicates that the magneto crystalline anisotropy, which is important to hold magnetic ions in certain direction, has been overcome by thermal energy [37]. The magnetic anisotropy constant is maximum for the concentration 0.8 and 0.6 with more crystallinity with no superstructure peaks are obtained. From these results magneto crystalline anisotropy is more for high crystallinity sample. And high crystallinity is possible in disordered spinel structure. Ordered spinel structure have low value of magnetic anisotropy constant. No sample in the present study have ordered structure. Thus VSM result matches with XRD, SEM and FTIR findings.

IV. Conclusion

$Co_xNi_{1-x}Cr_{0.5}Fe_{1.5}O_4$ (x = 0, 0.2, 0.4, 0.8, 1.0) nanoferrites were successfully synthesized by easy and simple co-precipitation method with average crystallite size between 39 nm and 60 nm. All physical properties are studied for samples sintered at 1173K. Addition of Co^{2+} ion influenced the structural properties such as Average crystallite size, lattice constant, lattice strain, dislocation density and X-Ray density of the synthesized samples. absence of super structure reflection peaks from XRD analysis suggest that nano crystal lattice having disordered spinel structure in the higher concentration of the dopant. SEM shows morphology manipulated by Co^{2+} ion in the sample and FTIR observation have fine match with results of XRD and SEM. From VSM analysis and Low concentration of Co^{2+} induced magnetic ordering and crystal disordering. At higher concentration Cobalt induced most disordered magnetic structure which is found from the magnetic anisotropy

constant value. Important finding in this work is 0.8 and 0.6 concentration of Cobalt in Ni-Cr in nano ferrite has its maximum magnetic anisotropy constant value, which will release more thermal energy in alternating magnetic field, and should be act as best candidate for magnetic fluid hyperthermia and in targeted drug delivery system.

References

[1]. H.Basti, L.B.Tahar, L.S.Smiri, F.Herbst, M.J.Vaulay, F.Chaus, S.Ammar and S.Benderbous, *J.Colloid interface Sci., 341* (2010) 248-254.
[2]. J.H.H.Wang, L.Ding, D.Li and Y.Han, *Appl.Surf.Sci, 257* (2011) 7107-7112.
[3]. K.Raju, G.Venkataiah and D.H.Yoon, *Ceram.Int., 40* (2014) 9337-9344.
[4]. S.Ramesh, B.Chandra Sekhar, P.S.V.S.Rao and B.P.Rao, *Ceram.Int., 40* (2014) 8729-8735.
[5]. S.H.Xuan, L.Y Hao, W.Q.Jiang, L.Song, Y.Hu, Z.Y.Chen, L.F.Fei and T.W.Li, *Cryst. Growth Des.,7* (2007) 430-434.
[6]. C.C. Berry, Progress in functionalization of magnetic nanoparticles for appli-cations in biomedicine, *J. Phys. D: Appl. Phys. 42* (2009) 224003.
[7]. B.D.Culity, *Elements of X-ray diffraction* Chapter 14 (London, Addison-Wesley publishing company.Inc.,1976) (Chapter 14).
[8]. C.Kittel, *Introduction to Solid State Physics* 7th ed (USA, John willey publishing company, 1956).
[9]. A.Goldman, *Modern Ferrite technology*, 2nd ed., (New York , Springer Science Business Media Inc., 2006).
[10]. M.Raghasudha, D.Ravinder, P.Veerasomaiah, *J.Magn.Magn., and Mater., 420* (2016) 45-50.
[11]. Mohd Mohsin Nizam Ansari, Shakeel Khan, *Physica B, 520* (2017) 21-27.
[12]. Bi-Yu Chen, Ding Chen, Zhi-tao kang, Ying-zhe Zhang, *J.Alloy and Comp., 618* (2015) 222-226.
[13]. Luderd.U, Bibes.M, Bouzehounane.K, Jacquet.E, Contour.J, P.Fusil, S.Bobo, *Appl.Phys.Lett.88*, 082505(2006)
[14]. T.F.Marinca, I.Chicinas, O.Isnard, V.Pop, F.Pop, *J.Alloy., and compounds, 509* (2011) 7931-7936.
[15]. S.R.Dhage, Y.Khollam, S.B.Deshpande, V.Ravi, *Mater.Res.Bulls. 378* (2003) 1601-1605.
[16]. C.G.Ammankutty., S.Sugunna, *J.App.Catal.A Gen 218* (2001) 39
[17]. Sepleak.V, Bergmann.I, Indris.S, Feldhoff.A, Hahn.H, Becker.K.D, *J.Mater. Chem 21* (2011) 8332
[18]. B.P.Ladgaonkar, A.S.Vaigainkar, *Materials chemisty and physics 56* (1998) 280-283.
[19]. C.S.Narasimhan and C.S. Swamy, *Physica status dolidi 59* (1980) 817
[20]. G.Sathishkumar., C.Venkataraju., K..Sivakumar, *Material Sciences and Applications 1* (2010) 19-24
[21]. E.Wolska, P.Piszora, W.Nowicki, J.Darul, *Int.J.Inorganic Mater., 3* (2001), 503-507.
[22]. G.K.Williamson, W.H.Hall , *Acta Metall.1*(1953) 22-31.
[23]. A.Kohrsand Zak, W.H.Abd.Majid, M.E. Abrishami, Ramin Yousefi, *Solid State Sci.13* (2011) 251-256.
[24]. Tan.X., Li, G., Zhao, Y., Hu, *C. Mater. Res. Bull.44*, (2009) 2160.
[25]. Singhal.J, Singh.S, Barthwal.K, Chandra.K, *Journal of solid state chemistry 178* (2005) 3183-3189.
[26]. S.Rahman, K.Nadeem, M.A.Rehman, M.Mumtaz, S.Naeem, I.L.Ipst,*Ceram.Int. 39* (2013) 5235-5239
[27]. S.Prabahar, and M.Dhanam, *J.Cryst.Growth, 41* 285 (2005) 1-2
[28]. Hashim.M, Alimuddin, Shirsath.S.E, Kumar.S, Kumar.R, Roy.A.S, Shah.J, and Kotnala.R.K, *Journal of alloys and compounds, 549* (2012) 348-357.
[29]. Farid.M, Ahmad.I, Aman.S, Kanwal.M, Murtaza.G, Alia.I, Ishfaq.M, *Journal of Ovonic research 11* (2015) 1
[30]. Wahba.A.M, Mohammad.M.B, *Ceramic International, 40* (2014) 6127-6135
[31]. Boshale.A.G, Chougule.B.K, *Material chemisty and physics 97* (2006) 273
[32]. Smit.J, And H.P.J ijn.*Ferrite* (1959)
[33]. Shirsath.S.E, Toksha.B.G, Kadam.R.H, PatangeS.M, Mane.D.R, Jangam.G.S, Ghasemi.A, *J.Physics chemistry of solids 71* (2010) 1669
[34]. Singh.N, Agrawal.A, Sanghi.S, Singh.P, *Physica B, 406* (2011) 687
[35]. Singhal.S, Chandra.K, *J.Solid state Chem. 180* (2007) 296
[36]. Gabbal.M.A, Angari.Y.M.A, *Material chem. Physics 118* (2009) 153
[37]. Verma.A, Goel.T.C, Meadiratta.R.G, Kishan.P, *Journal of Magnetism and magnetic material 208* (2000) 13-19.

Table 1: Comparison of X-Ray Intensity

Co content 'x'	Composition	I_{220}	I_{440}
0.0	$Ni_{1.0}Cr_{0.5}Fe_{1.5}O_4$	34.10	32.58
0.2	$Co_{0.2}Ni_{0.8}Cr_{0.5}Fe_{1.5}O_4$	35.34	43.44
0.4	$Co_{0.4}Ni_{0.6}Cr_{0.5}Fe_{1.5}O_4$	30.41	45.07
0.6	$Co_{0.6}Ni_{0.4}Cr_{0.5}Fe_{1.5}O_4$	37.61	34.93
0.8	$Co_{0.8}Ni_{0.2}Cr_{0.5}Fe_{1.5}O_4$	34.44	37.98
1.0	$Co_{1.0}Cr_{0.5}Fe_{1.5}O_4$	34.29	42.34

TABLE 2: Structural parameters of $Co_xNi_{1-x}Cr_{0.5}Fe_{1.5}O_4$ for various concentrations sintered at 1173K

Co content 'x'	Composition	Crystallite Size D (nm)	Lattice Constant a (Å)	Molecular Weight g/mole	X-ray density g/cm^3	Lattice strain 10^{-3}	Dislocation Density 10^{15}
0.0	$Ni_{1.0}Cr_{0.5}Fe_{1.5}O_4$	44.74	8.4407	232.405	5.1340	2.48	1.68
0.2	$Co_{0.2}Ni_{0.8}Cr_{0.5}Fe_{1.5}O_4$	54.10	8.4886	232.453	5.0487	2.26	0.85
0.4	$Co_{0.4}Ni_{0.6}Cr_{0.5}Fe_{1.5}O_4$	60.00	8.5172	232.501	4.9990	1.70	0.54
0.6	$Co_{0.6}Ni_{0.4}Cr_{0.5}Fe_{1.5}O_4$	39.40	8.5410	232.549	4.95835	4.08	2.94
0.8	$Co_{0.8}Ni_{0.2}Cr_{0.5}Fe_{1.5}O_4$	46.70	8.5209	232.597	4.9946	2.63	1.16
1.0	$Co_{1.0}Cr_{0.5}Fe_{1.5}O_4$	60.30	8.5328	232.645	4.9749	1.69	0.50

TABLE 3: Vibrational frequency of tetrahedral and octahedral sites

Co content 'x'	Composition	$\nu_{1\ tetra}$	$\nu'_{1\ tetra}$	$\nu_{2\ octa}$	$\nu'_{2\ octa}$
0.0	$Ni_{1.0}Cr_{0.5}Fe_{1.5}O_4$	614.01	495.76	443.25	-
0.2	$Co_{0.2}Ni_{0.8}Cr_{0.5}Fe_{1.5}O_4$	616.94	-	440.40	418.22
0.4	$Co_{0.4}Ni_{0.6}Cr_{0.5}Fe_{1.5}O_4$	613.15	-	442.79	-
0.6	$Co_{0.6}Ni_{0.4}Cr_{0.5}Fe_{1.5}O_4$	611.76	-	-	419.45
0.8	$Co_{0.8}Ni_{0.2}Cr_{0.5}Fe_{1.5}O_4$	608.36	-	435.38	419.12
1.0	$Co_{1.0}Cr_{0.5}Fe_{1.5}O_4$	601.64	-	432.39	-

TABLE 4: Magnetic parameters of $Co_xNi_{1-x}Cr_{0.5}Fe_{1.5}O_4$ for various concentrations sintered at 1173K

Co content 'x'	Composition	M_s (emu/g)	M_r (emu/g)	H_c (Oe)	M_r/M_s	K (erg/cm^3)	n_B
0.0	$Ni_{1.0}Cr_{0.5}Fe_{1.5}O_4$	29.21	13.21	316.5	0.452	9244.97	1.215497
0.2	$Co_{0.2}Ni_{0.8}Cr_{0.5}Fe_{1.5}O_4$	32.14	17.48	322.1	0.544	10352.29	1.337697
0.4	$Co_{0.4}Ni_{0.6}Cr_{0.5}Fe_{1.5}O_4$	31.57	18.89	255.4	0.598	8062.98	1.314245
0.6	$Co_{0.6}Ni_{0.4}Cr_{0.5}Fe_{1.5}O_4$	80.38	45.03	166.6	0.560	13391.31	3.346874
0.8	$Co_{0.8}Ni_{0.2}Cr_{0.5}Fe_{1.5}O_4$	73.84	36.20	233.2	0.490	17219.49	3.075195
1.0	$Co_{1.0}Cr_{0.5}Fe_{1.5}O_4$	61.73	13.12	166.6	0.213	10284.22	2.57138

M_s - Saturation magnetization; M_r - Remanent Magnetization; H_c – Coercivity; K - Magneto Crystalline Anisotropy; n_B-Magneton Number

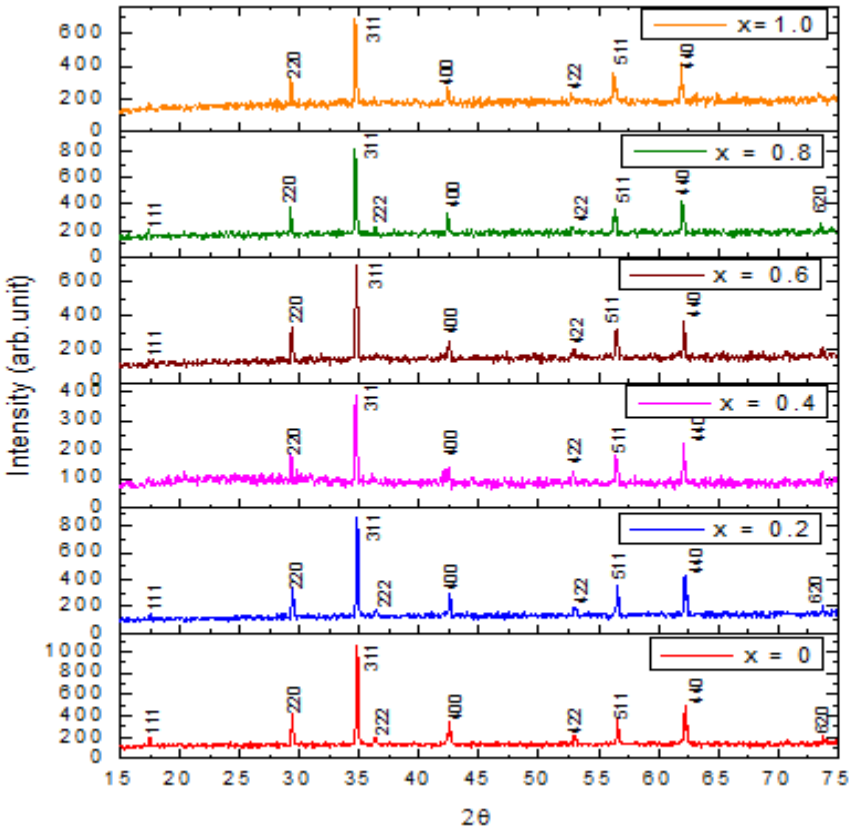

Figure 1: X-Ray Diffraction pattern of Co Doped Ni-Cr nano ferrite samples

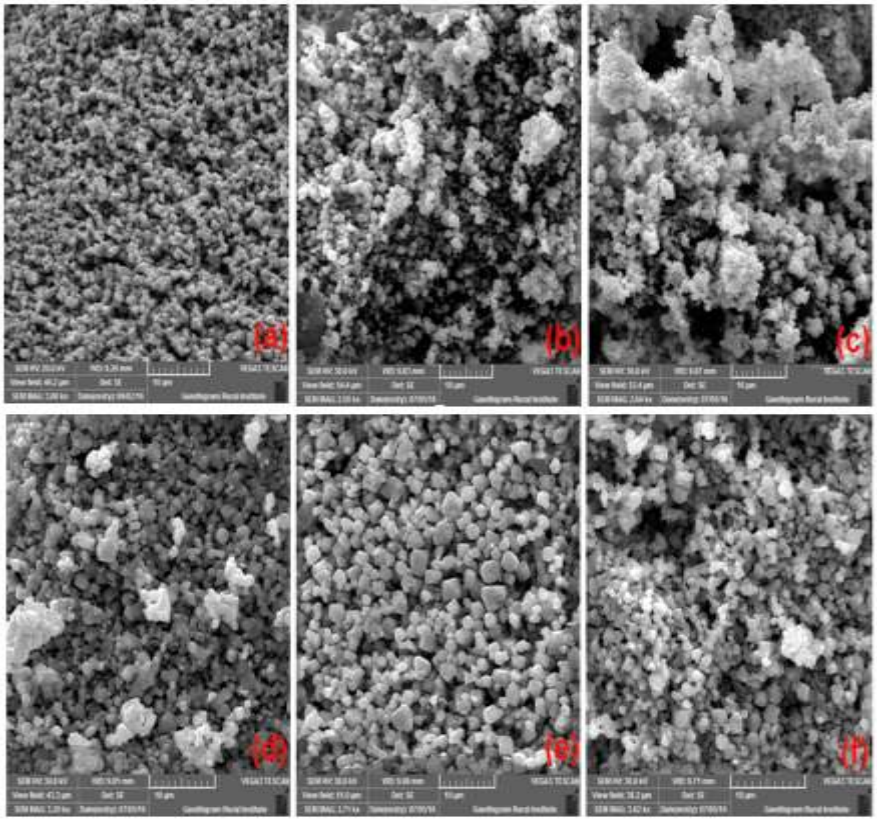

Figure 2. SEM micrograph of $Co_xNi_{1-x}Cr_{0.5}Fe_{1.5}O_4$ (x= 0(a), 0.2(b), 0.4(c), 0.6(d), 0.8(e), 1.0(f)) nanoferrite sintered at 1173K

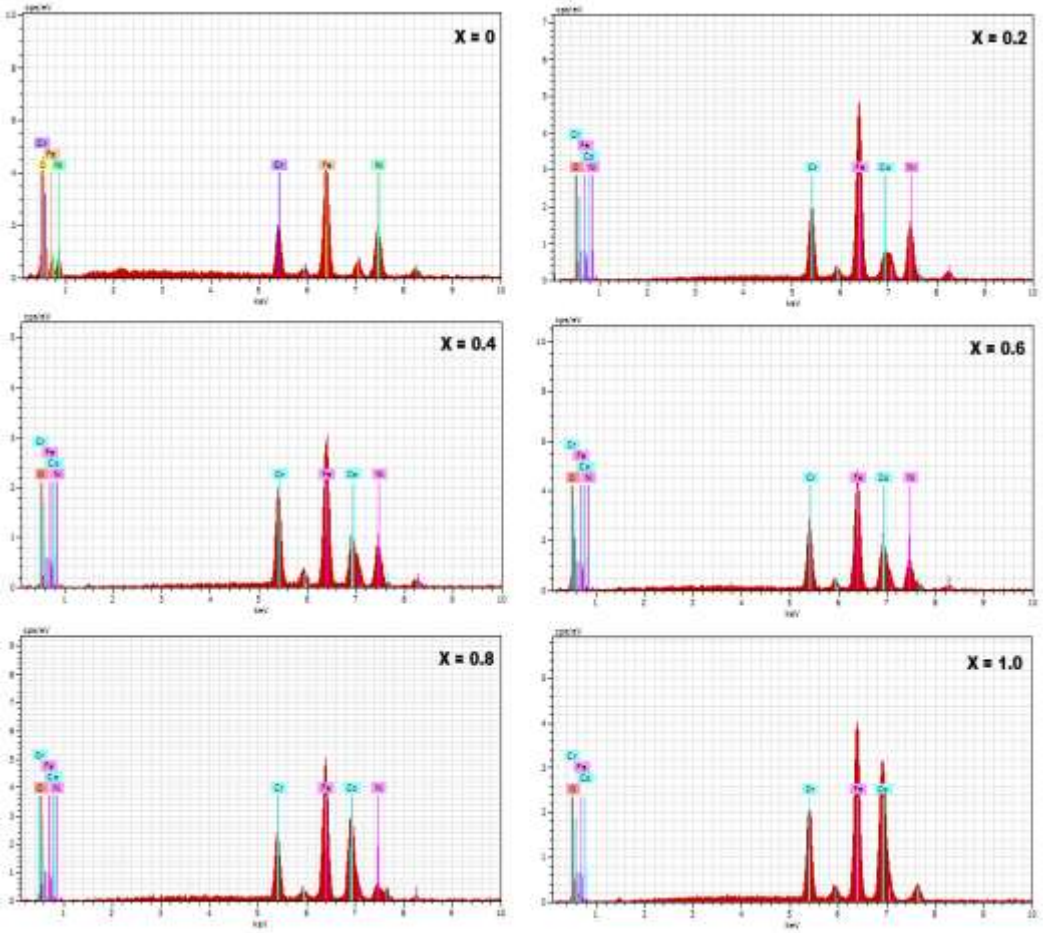

Figure 3. EDS of $Co_xNi_{1-x}Cr_{0.5}Fe_{1.5}O_4$ (x= 0,0.2, 0.4, 0.6, 0.8, 1.0) nanoferrite sintered at 1173K

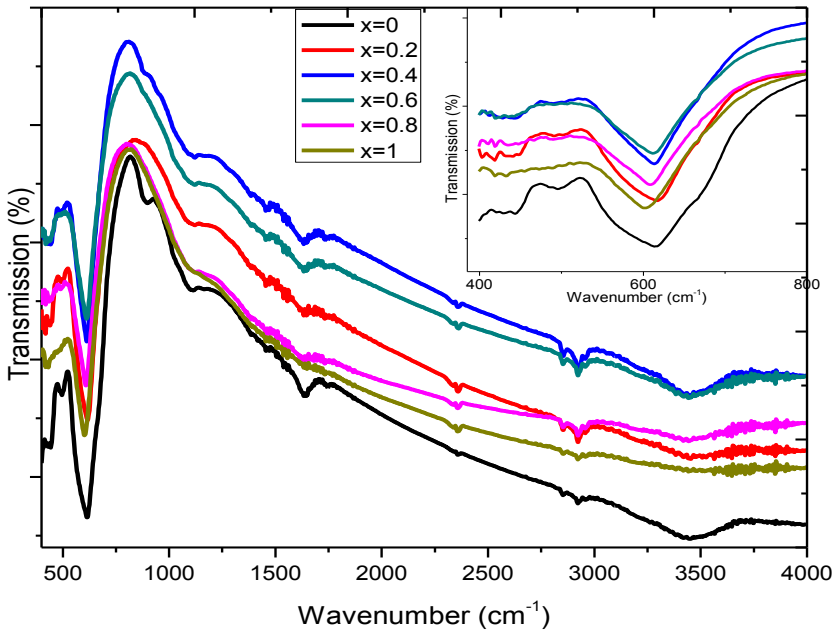

Figure 4. FTIR spectra of $Co_xNi_{1-x}Cr_{0.5}Fe_{1.5}O_4$ (x= 0,0.2, 0.4, 0.6, 0.8, 1.0) nanoferrite sintered at 1173K

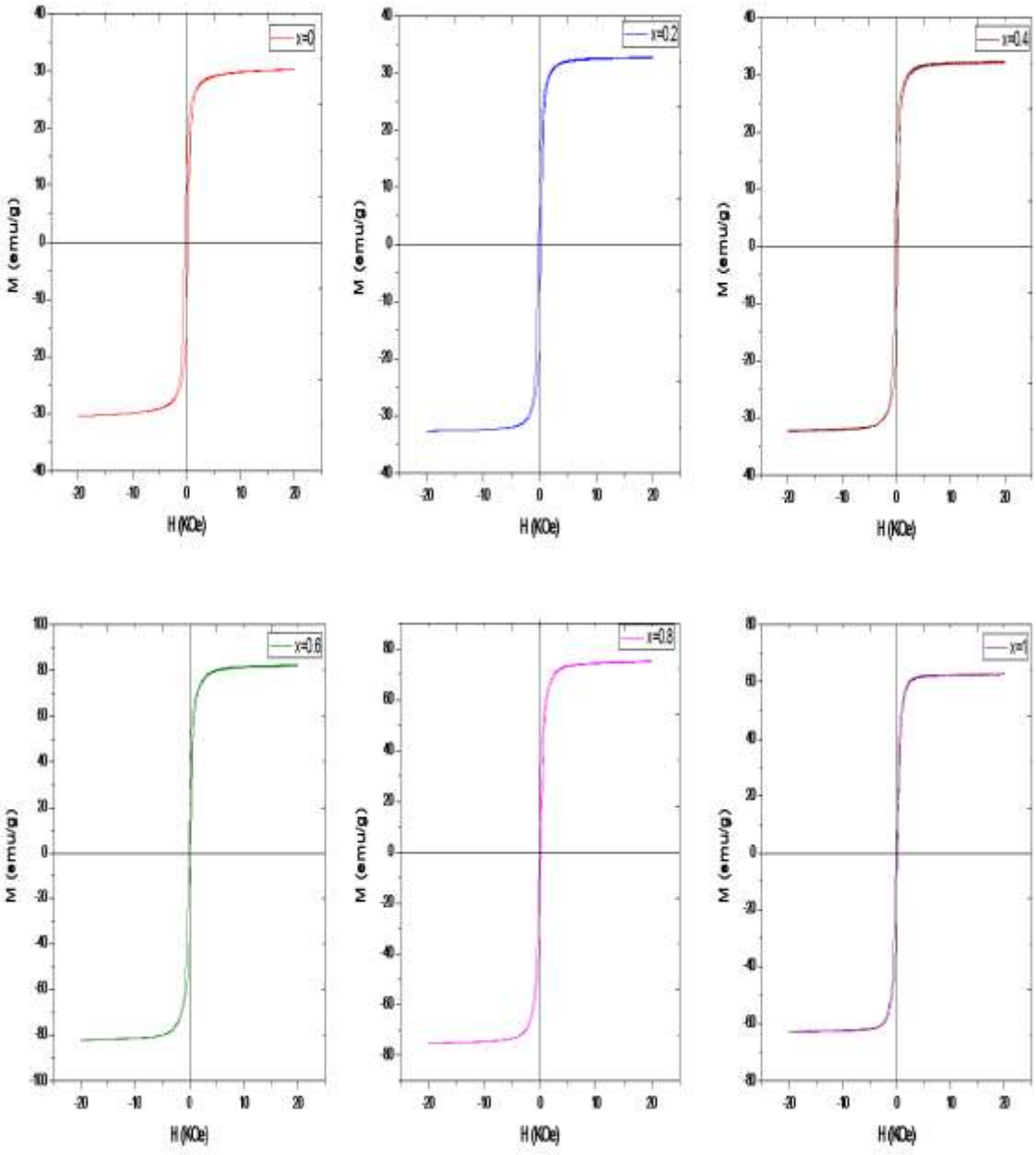

Figure 5. Magnetic hysteresis curves of $Co_xNi_{1-x}Cr_{0.5}Fe_{1.5}O_4$ (x= 0,0.2, 0.4, 0.6, 0.8, 1.0) sintered at 1173K

IOSR Journal of Applied Physics (IOSR-JAP) is UGC approved Journal with Sl. No. 5010, Journal no. 49054.

S. Sukandhiya. "Influence of Co2 ions on structural and magnetic properties of Co-Precipitated Ni-Cr nanoferrite." IOSR Journal of Applied Physics (IOSR-JAP) , vol. 9, no. 4, 2017, pp. 04–12.